

ACCEPTED MANUSCRIPT • OPEN ACCESS

Present and future land surface and wet bulb temperatures in the Arabian Peninsula

To cite this article before publication: Sarah Safieddine *et al* 2022 *Environ. Res. Lett.* in press <https://doi.org/10.1088/1748-9326/ac507c>

Manuscript version: Accepted Manuscript

Accepted Manuscript is “the version of the article accepted for publication including all changes made as a result of the peer review process, and which may also include the addition to the article by IOP Publishing of a header, an article ID, a cover sheet and/or an ‘Accepted Manuscript’ watermark, but excluding any other editing, typesetting or other changes made by IOP Publishing and/or its licensors”

This Accepted Manuscript is © 2022 The Author(s). Published by IOP Publishing Ltd.

As the Version of Record of this article is going to be / has been published on a gold open access basis under a CC BY 3.0 licence, this Accepted Manuscript is available for reuse under a CC BY 3.0 licence immediately.

Everyone is permitted to use all or part of the original content in this article, provided that they adhere to all the terms of the licence <https://creativecommons.org/licenses/by/3.0>

Although reasonable endeavours have been taken to obtain all necessary permissions from third parties to include their copyrighted content within this article, their full citation and copyright line may not be present in this Accepted Manuscript version. Before using any content from this article, please refer to the Version of Record on IOPscience once published for full citation and copyright details, as permissions may be required. All third party content is fully copyright protected and is not published on a gold open access basis under a CC BY licence, unless that is specifically stated in the figure caption in the Version of Record.

View the [article online](#) for updates and enhancements.

1 Present and future land surface and wet bulb temperatures in the Arabian Peninsula

2 S. Safieddine¹, C. Clerbaux^{1,2}, L. Clarisse², S. Whitburn², and E.A.B. Eltahir³,

3 ¹*LATMOS/IPSL, Sorbonne Université, UVSQ, CNRS, Paris, France*

4 ²*Université libre de Bruxelles (ULB), Spectroscopy, Quantum Chemistry and Atmospheric*
5 *Remote Sensing (SQUARES), Brussels, Belgium*

6 ³*Ralph M. Parsons Laboratory, Massachusetts Institute of Technology, Cambridge, MA*
7 *02139, USA*

8 Abstract

9
10 The Arabian Peninsula exhibits extreme hot summers and has one of the world's largest
11 population growth. We use satellite observations and reanalysis as well as climate model
12 projections to analyze morning and evening land surface temperatures (LST), to refer to
13 processes at the surface, and wet bulb temperatures (WBT) to measure human heat
14 stress. We focus on three regions: The Persian Gulf and Gulf of Oman, the inland capital
15 of Saudi Arabia, Riyadh and the irrigated agricultural region in Al-Jouf, Saudi Arabia. This
16 study shows that the time of the day is important when studying LST and WBT, with
17 current and future WBT higher in the early summer evenings. It also shows that the effect
18 of humidity brought from waterbodies or through irrigation can significantly increase heat
19 stress.

20 Over the coasts of the Peninsula, humidity decreases LST but increases heat stress via
21 WBT values higher than 25°C in the evening. Riyadh, located in the heart of the Peninsula
22 has lower WBT of 15°C to 17.5°C and LST reaching 42.5°C. Irrigation in the Al-Jouf
23 province decreases LST by up to 10° with respect to its surroundings, while it increases
24 WBT by up to 2.5°. Climate projections over the Arabian Peninsula suggest that global
25 efforts will determine the survivability in this region. The projected increase in LST and
26 WBT approaches +6° and +4°C respectively in the Persian Gulf and Riyadh by the end of
27 the century, posing significant risk on human survivability in the Peninsula unless strict
28 climate mitigation takes place.

29 Key words:

30 Arabian Peninsula, land surface temperature, wet bulb temperature, extreme heat, IASI,
31 ERA5, Climate projections, EC-Earth

32 Significance statement

33 The Arabian Peninsula is exhibiting fast economic and social development. It is
34 surrounded by seas, bringing humidity to the coasts but also has the largest desert in
35 Asia. This contrast is investigated using the land and wet bulb temperatures. The first is

1
2
3 36 linked to surface while the second is a measure of human heat stress. Results are
4 37 alarming and show that unless global efforts are made to reduce climate change,
5 38 survivability in this regions by mid to end of the century is threatened. Irrigation will
6 39 enhance the heat stress through the increase in humidity, and the “greening” efforts need
7 40 to be considered carefully. Interestingly, current and future heat stress is more prominent
8 41 in the early evenings, when people go out.

12 42 **1. Introduction**

14 43 Most land regions are experiencing greater warming than the global average temperature
15 44 increase¹, and the projections of future temperatures have large regional and local
16 45 uncertainties since models fail in the representation of local land processes². This poses
17 46 some important limitations on the accuracy of these projections on a local scale and as
18 47 such, their societal/epidemiological impacts such as those of temperature extremes³.
19 48 From here stems the need to understand the important variables for the feedback between
20 49 land and atmosphere, and their effect on human survivability under extreme heat
21 50 conditions. We present here two variables that can help us understand this complex
22 51 relationship in a region with extreme heat in summer, the Arabian Peninsula: the land
23 52 surface temperature (LST) and the wet bulb temperature (WBT).

28 53 LST relates to the thermal radiation emitted by the Earth’s surface, from depths as small
29 54 as 10–20 micrometers⁴. It is usually obtained from remote sensing data. Differences
30 55 between LST and atmospheric near surface temperature can be large under cloud-free,
31 56 low wind speed conditions since land heats much faster than air, and smaller under cloudy
32 57 conditions or when solar insolation is low⁵. It is an important factor for studying the Earth’s
33 58 energy balance, convection at the surface, monitoring droughts, land use, and surface
34 59 urban heat islands (SUHI)^{6,7}. SUHIs exist when the temperature of the surface is warmer
35 60 in urban areas than in rural surroundings⁸. The inverse phenomenon is the surface urban
36 61 cool island (SUCI) effect and is common to dry and arid climate: the city is cooler than its
37 62 surrounding. This has been detected in many cities in dry climates around the world⁹, and
38 63 in many metropolitans of the Arabian Peninsula, such as the cities of Kuwait¹⁰, Riyadh¹¹,
39 64 or Dubai⁹. Sand’s temperature can be extremely high during sunny summer days: it has
40 65 very low water content and a fast depletion rate of water via evaporation. Sand holds less
41 66 water than other materials and has smaller thermal inertia. Over the surface, low relative
42 67 humidity enhances the dryness and heat exacerbating soil aridity in the upper layers of
43 68 the sand. LST has been identified as one of the most significant factors that can influence
44 69 SUHI/SUCI phenomena^{12,13}. Studies have shown that urban development incorporating
45 70 vegetation could be a primary strategy to mitigate SUHI¹⁴. However, vegetation, especially
46 71 in arid regions, requires irrigation, which adds humidity to the atmosphere. Humidity is
47 72 also brought naturally from the sea to coastal regions, and the Arabian Peninsula is
48 73 surrounded by bodies of water: The Red Sea to the west and southwest, the Persian Gulf
49 74 and the Gulf of Oman to the northeast, and the Arabian Sea and the Indian Ocean to the

southeast. A good metric to assess the combined effect of humidity and temperature to the coasts of the peninsula is the wet bulb temperature, WBT. It depends both on air temperature (also called dry bulb temperature) and air humidity near the surface. It is important in the context of extreme heat, as it reflects the body's limited ability to efficiently shed heat. Heat episodes with high WBT can be dangerous to human's health and lower productivity of outdoor laborers^{15,16}. Any exceedance of 35 °C for extended periods will induce hyperthermia as dissipation of body metabolic heat becomes impossible. It is therefore a measure of heat stress and current available observations show that it rarely exceeds 31 °C¹⁷.

The Arabian Peninsula is a region of extreme heat in summer, and is a center of demographic, and urban development as it is the world's single largest source of petroleum. Economic expansion in countries like Saudi Arabia, United Arab Emirates (UAE), Kuwait, Oman, Qatar and Bahrain has encouraged millions of migrants to move to the Middle East for work. Under climate change stress, and the influx of population to this region, this study aims at understanding the effect of geographical location and land use and on the current and future summer (June, July August, JJA) heat stress, during day and night separately, and their implications, which should be taken into account in urban development strategies.

2. Methods

2.1. IASI Land Surface Temperature

The LST product used in this work is provided by the family of the Infrared Atmospheric Sounding Interferometer (IASI) instruments¹⁸, on board of the Eumetsat (European Organisation for the Exploitation of Meteorological Satellites) Metop series of polar orbiting satellites: Metop-A, launched in 2006, Metop-B launched in 2012, and Metop-C launched in 2018. Each instrument has a morning and an evening orbit at around 9:30 AM and PM. IASI measures calibrated radiances in the thermal infrared spectral range, at a global scale and revisiting all points on the Earth's surface twice a day. In spectral bands where no gas absorbs, accurate information on the surface properties and temperature is derived. The latter is clear-sky product retrieved using a method based on entropy reduction/information theory and neural networks¹⁹. Validation of this product with other datasets (satellite and ground-based measurements) shows that it is suitable for trend analysis and to check for local and regional variations of temperature in different regions of the world¹⁹. In order to achieve a higher resolution for spatial coverage, we averaged the IASI LST using an oversampling method, widely used in other studies for various trace gases concentrations using different instruments²⁰⁻²² but until now, never for temperature analysis with IASI. The three instruments are cross validated for temperature and show excellent agreement²³. Metop-A has been decommissioned in 2017. In this work, a combination of the three instruments' products is used for summers of 2008 to 2020.

2.2. Wet bulb temperature

1
2
3 114 The wet bulb temperature is a nonlinear function of temperature and humidity near the
4 115 surface. In this work we use the formula of WBT provided by Davies-Jones²⁴. Near surface
5 116 temperature and humidity used to calculate WBT are provided by the European Center
6 117 for Medium Weather Forecast (ECMWF)'s latest reanalysis ERA5²⁵. ERA5 datasets are
7 118 at $0.25^\circ \times 0.25^\circ$ resolution (native horizontal resolution of ERA5 is $\sim 31\text{km}$). All different
8 119 retrieved variables are interpolated in time and space to match the IASI morning and
9 120 evening observations. We do not use the LST from ERA5, since the super sampling
10 121 method of IASI data leads to much finer resolution (of around $0.01^\circ \times 0.01^\circ$) as the figures
11 122 1 to 3 show. ERA5 assimilates IASI radiances, and the two datasets agree very well as
12 123 shown by Safieddine et al., 2020 and Bouillon et al., 2020.

17 124 **2.3. EC-Earth Climate model**

19 125 The reanalysis uses the ECMWF's Integrated Forecasting System for the atmosphere–
20 126 land component (IFS). IFS is also used by the European Earth Consortium climate model
21 127 (EC-Earth, <http://www.ec-earth.org/>). It is complemented with other model components to
22 128 simulate the full range of Earth system interactions that are relevant to climate²⁶. The
23 129 model participates in CMIP6²⁷ (Climate model intercomparison project, phase 6, part of
24 130 the Intergovernmental Panel on Climate Change (IPCC) report of 2021¹) with different
25 131 model configurations. Here we use the Scenario Model Intercomparison Project
26 132 (ScenarioMIP), covering the period [2015- 2100]. We note that the versions of the IFS
27 133 models used in ERA5 and in EC-Earth are not identical. EC-Earth branched off to include
28 134 its own additions for climate purposes. Moreover, EC-Earth is not assimilated and is not
29 135 initialized with observations several times a day like ERA5. We do not attempt to validate
30 136 therefore EC-Earth with ERA5. In this work, we use the simulations from two shared socio-
31 137 economic pathways (SSP)²⁸: the SSP2-4.5 corresponds to “middle of the
32 138 road/sustainability” socio-economic family with a nominal 4.5W/m^2 radiative forcing level
33 139 by 2100, and the SSP5-8.5 (8.5 W/m^2) marks the upper edge of the SSP scenario
34 140 spectrum with a high reference scenario in a high fossil-fuel development world throughout
35 141 the 21st century.

43 142 **3. Results**

44 143 **3.1. Local diurnal variation of land surface and wet bulb temperatures**

46 144 The Arabia Peninsula is well-targeted since the cloud cover over this region during
47 145 summer is negligible, giving IASI frequent access to the surface in order to derive clear-
48 146 sky LST. We focus on the summer season since it is the most relevant for human heat
49 147 stress. We calculate WBT from the ERA5 temperature and humidity interpolated in time
50 148 and space to the IASI morning and evening available observations (9:30 AM and PM). We
51 149 focus on three distinct regions: the first is coastal, the Persian Gulf and the Gulf of Oman.
52 150 The second is Riyadh, the capital of Saudi Arabia, $\sim 500\text{ km}$ away from the coast, and the

1
2
3 151 third is a large agricultural region in Saudi Arabia, in al-Jouf province. The location of the
4 152 three region is shown in Figure 4, panel (i).

6 153 **3.1.1. The Persian Gulf and the Gulf of Oman**

8 154 Figure 1 shows the morning (labeled “Day”) and evening (“Night”) land surface and wet
9 155 bulb temperature over the Persian Gulf and the Gulf of Oman. We chose this region
10 156 because it has major coastal cities (such as Sharjah, Dubai, and Abu Dhabi) with high
11 157 population densities, and the city of Al-Ain which is a major in-land city of the Abu Dhabi
12 158 province. The LST is 40 to 45°C close to the coasts, lower than the inland values as the
13 159 sea breeze transfers cooler air to the adjacent areas of the coast and enhances wind
14 160 speed. LST is higher during the day, and smaller during the summer nights, since it is
15 161 largely dependent on solar radiation. LST increases as the distance from the coast
16 162 increases, approaching 50°C during the day and 35°C during the night. We note that other
17 163 factors can play a significant role in increasing or decreasing LST, including elevation, and
18 164 the presence of green areas¹¹.

23 165 The WBT for the coastal cities (23° to 26°C) is much higher than the inland WBT both
24 166 during the day and the night. The city of al-Ain for example, has high LST but a WBT lower
25 167 by 3° to 6° than those recorded at the coastal cities. This clearly shows the dependence
26 168 of the WBT on the relative humidity (and time of the day). In the evening, the heat stress
27 169 (WBT) is higher since it corresponds to around 9:30 PM, with land-sea exchanges
28 170 saturating the air with humidity, affecting human’s heat comfort during population leisure
29 171 time.

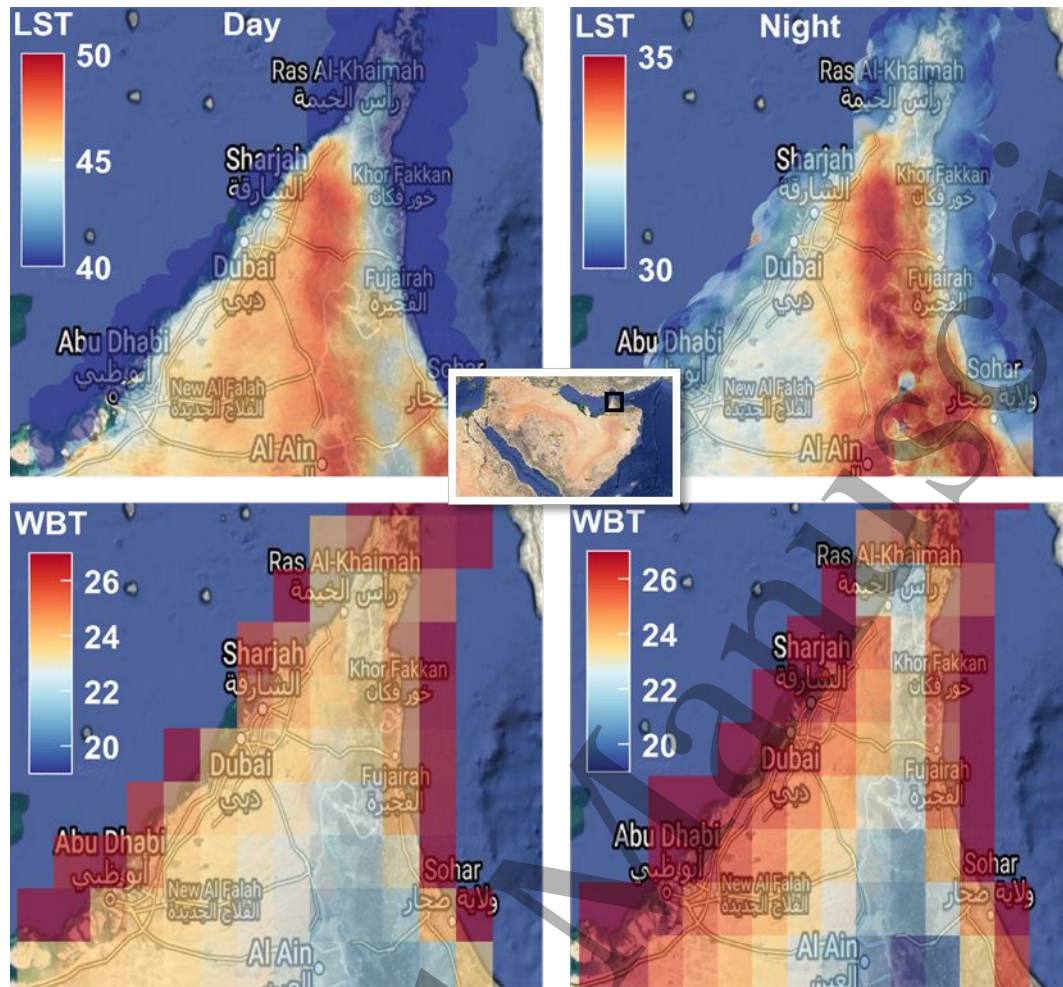
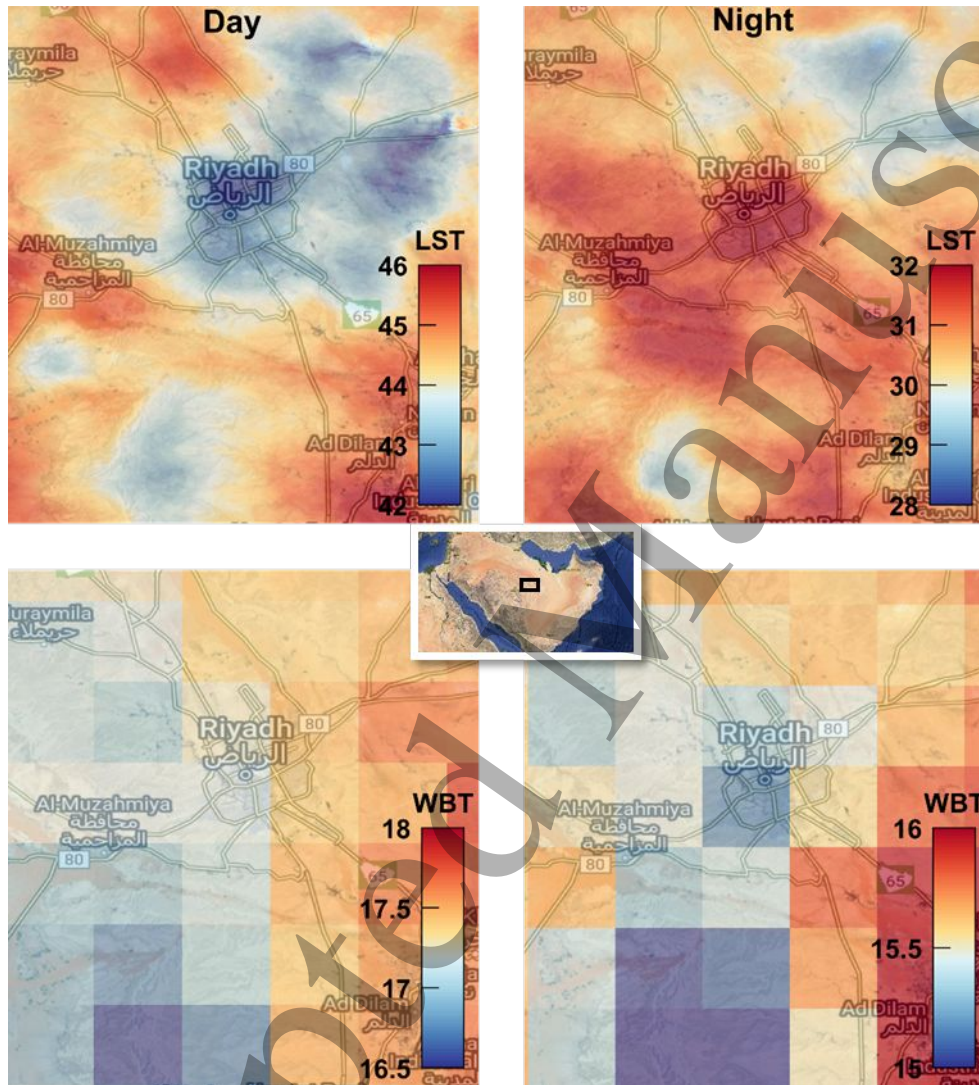


Figure 1. Upper panel: IASI day and night observations of LST during summer (June, July and August) for the cities on the Persian Gulf and the Gulf of Oman. Lower panel: ERA5 Wet Bulb Temperature interpolated to the time and location of IASI's observation. Note that the color bar limits for LST differ in each of the panels.

3.1.2. Riyadh

In Figure 2, we show the day and night LST and WBT over Riyadh as an example of non-coastal city. Riyadh, during the day, acts as a SUCI, as the upper left panel of Figure 2 shows. With high solar radiation in summer, the desert sand becomes very hot. However, the city's landscape is cooler. This has been seen in previous studies for Riyadh, using different other instruments^{11,29}. At night, the desert/arid regions cool faster than the urban city, and Riyadh becomes a typical SUHI. In most climates, including arid regions, SUHI are prominent at night because street canyons tend to trap heat in addition to urban materials that have slower nighttime cooling rate than natural surfaces⁹. The lower panel shows the WBT calculated from ERA5. In-situ measurements of wet bulb temperatures recorded a summer average of 18.8°C ³⁰. We can see that the derived WBT here is slightly lower, probably due to the grid size (31 km), and is of $17\text{-}17.5^{\circ}\text{C}$ in the morning of summer

189 days, and between 15 and 16°C during summer nights. The resolution of ERA's WBT,
 190 while the best available reanalysis resolution available today, does not show a
 191 hotspot/coolspot concentrated over Riyadh itself. Nevertheless, the low humidity, which is
 192 common for in-land regions such as Riyadh, makes the heat stress, reflected in the WBT,
 193 lower on average. This is even recorded at night, when Riyadh acts as a SUHI.



195
 196 **Figure 2.** Same as Figures 1 but for Riyadh. The capital is located in the desert of the
 197 Arabian Peninsula and acts as an urban cool island during the day and as an urban heat
 198 island during the night. WBT values are lower than those over the Persian Gulf. Note that
 199 the limits of the temperature scales vary in each of the panels.

3.1.3. Al-Jouf agricultural region

Al-Jouf is characterized by hot desert climatic conditions and is one of the largest agricultural regions in Saudi Arabia. Agriculture in this region is heavily irrigated and primarily depends on limited nonrenewable groundwater sources³¹. This irrigation therefore affects the surface and near-surface properties that are reflected in Figure 3 with the LST and WBT. Since the fields are irrigated, LST is lower. The soil has higher water content which cools the surface. Vegetation also increases latent heat flux to the atmosphere through increased evaporative surface area and transpiration¹⁴. This is particularly clear over the center of this cultivated parcel of land shown in Figure 3. Over the whole domain, LST is lower at night, due to the lack of solar radiation heating the surface. Analysis of LST during each of the summer months (not shown here), suggests that irrigation is broadly constant all summer long over all of the crops shown here, as the region accounts for a numerous distinct variety of crops (Sdurayhem, 2019). On the other hand, the lower panel with the WBT shows an opposite effect: the heat stress is higher with higher WBT above and near the agricultural fields. This is mainly driven by the higher relative humidity from irrigation over the fields. Higher humidity and smaller temperatures over the fields makes the WBT humidity-limited. This is particularly seen during the day, as irrigation is recommended in the early morning, when temperature and wind speed are the lowest³³. Humidity in this case plays a big role in determining the heat comfort near irrigated land. On average, the figure shows that irrigation can increase the heat stress by 2-3° with respect to its surrounding.

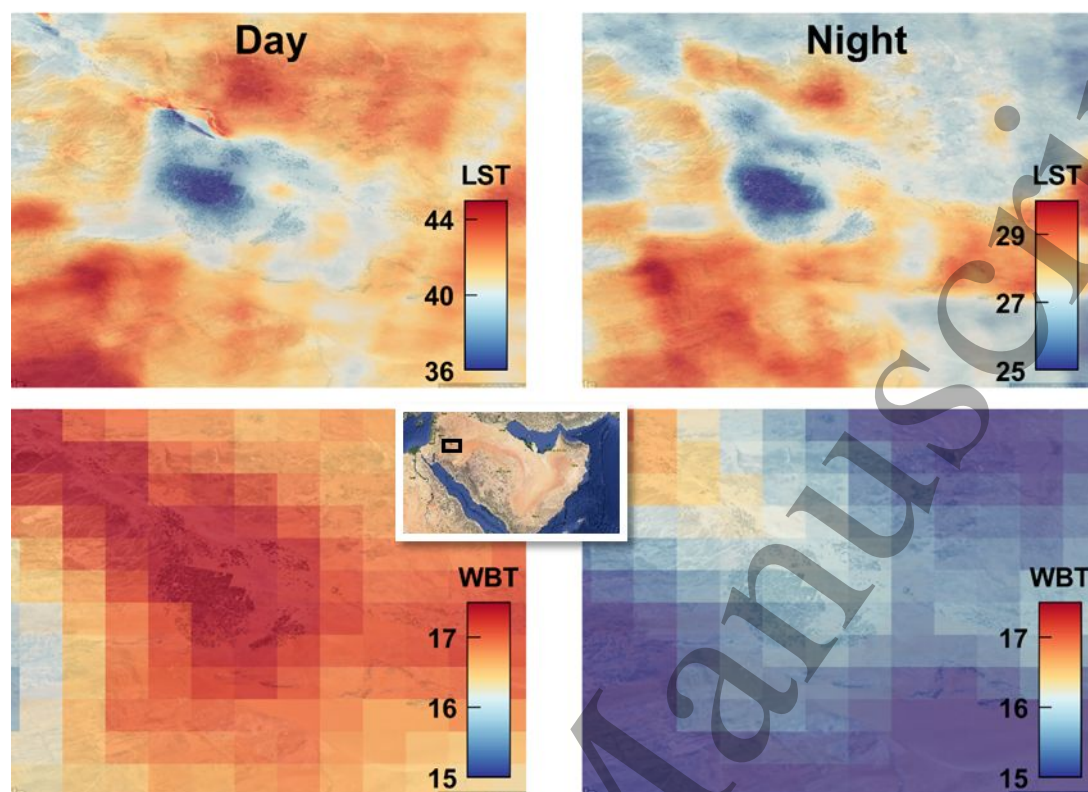


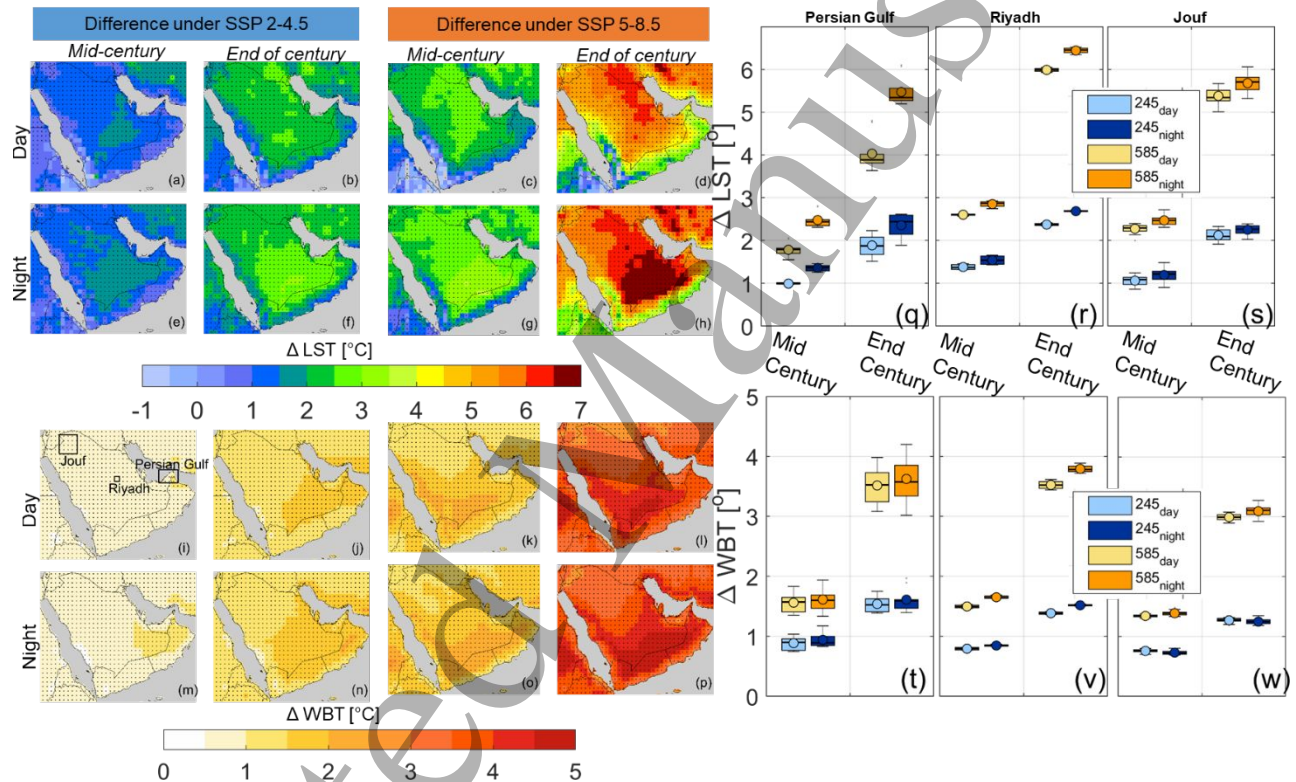
Figure 3. Same as Figures 1 and 2 but for the Al-Jouf agricultural region. Irrigation decreases LST but increases the heat stress through the increase in humidity near the surface.

4. Mid- to end century projections of regional LST and WBT

We focus now on the mid to end of century evolution of the summertime LST and WBT over this region under a “sustainable future” scenario (SSP 2-4.5) and a “fossil fuel development” SSP 5-8.5 scenario (section 2.3). With this, we can check the climate response of the present day observations/reanalysis of LST and WBT from IASI and ERA5 to different mitigation strategies. In fact, we do not attempt to validate the “present day” EC-Earth with that from IASI or ERA5 since over each of the 3 regions studied in Section 3, the local fine land processes might not be represented in the model. The urban heat/cool island effect or coast/land interaction in Riyadh and the Persian Gulf are much smaller than the model resolution (which is around $0.7^\circ \times 0.7^\circ$), and irrigation in Al-Jouf is not included in EC-Earth (as for many other climate models). Irrigation forecast remains very challenging as it depends on the evolution of soil, vegetation, water availability, expansion and shifts of agricultural practices. This clearly limits its ability to predict future WBT in al-Jouf and more generally everywhere else in the Peninsula. Moreover, the spatial resolution of the ERA5 or the EC-Earth dataset might not capture all meso- and

243 micro-scale variations of meteorological conditions, such as mesoscale convective
 244 systems³⁴, especially in areas with a complex orography, land cover, or near the coasts
 245^{35,36}. Even at the smallest grid cell, the simulation output is a collection of values averaged
 246 over an area. As such, it depends on grid cell size, the terrain complexity and the type of
 247 surface.

248 For all these reasons, the simulation used here, will tell us the climate response on the
 249 longer term without taking into account local land use changes. Since we calculate the
 250 difference between different climate periods, the increase can therefore be projected onto
 251 present-day values from IASI and ERA5.



252
 253 **Figure 4.** Panels a to p: mean change in day and night LST (upper panels) and WBT
 254 (lower panels) in mid-century [2045-2069] and end of century [2075-2099] with respect to
 255 the present day [2015-2039], under two different socio-economic pathways from the EC-
 256 Earth model. The dotted areas indicate statistical significance with 95 % confidence from
 257 a Student's *t* test. Panels q to w: box plot of the mean change in LST and WBT in the 3
 258 regions discussed in the study (locations are shown on panel (i)). The central black line
 259 indicates the median, the circle is the mean, and the bottom and top edges of the box
 260 indicate the 25th and 75th percentiles. The whiskers extend to the most extreme data.

261 We show in Figure 4 the mean change during the day (morning 3-hr average,
 262 corresponding to 9 to 12pm local time) and during the night (3-hr average, from 9pm to

1
2
3 263 midnight local time) of LST and WBT in the 25-year average climate representing mid-
4 264 century [2045-2069] and that at the end of the century [2075-2099] with respect to
5 265 present day climate [2015-2039] under 2 different SSPs. The end of century increase in
6 266 SSP2-4.5 is relatively close to that reached by mid-century for SSP5-8.5. . The latter
7 267 shows a grim increase in 2100 reaching +7° for LST (panels d and h) and +5° (panels l
8 268 and p) for WBT respectively, in southern Saudi Arabia and northern Oman and Yemen.
9 269 What can be noted is that the future increase in LST and WBT can be higher at night than
10 270 during the day. By the early evening, land would have stored all the heat from sunlight
11 271 (high LST) and the atmosphere in coastal areas would have been also saturated with
12 272 moisture (high temperature and humidity).

13
14
15
16
17 273 Panels *q* to *w* show the same mean change for the regions discussed in Section 3
18 274 (rectangles in panel *i*): The Persian Gulf, Riyadh, and Al-Jouf. The average increase in
19 275 summertime LST and WBT is more or less of the same magnitude for the three regions
20 276 in particular for the SSP2-4.5 scenario. This is due to the fact that the we are checking the
21 277 regional climate response. Moreover, relative humidity remains mostly constant over this
22 278 region under the different SSPs; a result that is expected on climatological time
23 279 scales^{1,37,38}, particularly over mid-latitude regions of the Northern Hemisphere. Therefore,
24 280 the increase in WBT is temperature-limited and as such is similar in regions close in
25 281 latitudes.

26 282 Panels *q* to *w* show that for the SSP2-4.5 scenario, and by mid-century, the increase in
27 283 LST for the 3 regions is between +1 and 1.6, and lower than +1°C for WBT for all three
28 284 regions (median values). By the end of the century, and for the same scenario, the
29 285 increase in LST is between +2°C and +3°C and is close to +1.5°C for WBT. The increase
30 286 in LST is much more enhanced for the SSP5-8.5 scenario. By mid-century, it is between
31 287 +1.8°C (day, Persian Gulf) and +3 °C (day, Riyadh). For WBT, it is between +1 and +2°C
32 288 for the three regions investigated (median values). In 2100, LST reaches an increase
33 289 close to or larger than +6° (Riyadh, at night), and WBT increases by more than +3° for all
34 290 the regions investigated. LST and WBT are both higher in the evening than in the morning.
35 291 This increase in WBT in the Persian Gulf and the Gulf of Oman would make average WBT,
36 292 as compared to Figure 1, close to or higher than 30°C. An increase of this magnitude in
37 293 WBT would possibly lead to premature death of the weakest, namely children and
38 294 elderly¹⁷.

39
40
41
42
43
44
45
46
47
48 295

49 296 **Discussion and Conclusions**

50
51
52 297 We investigate in this study the current and future LST and WBT over the Arabian
53 298 Peninsula. Using high resolution LST observations from IASI satellite measurements and
54 299 WBT calculated from reanalysis data from ERA5, the hottest temperatures recorded

1
2
3 300 during the summer days are those over the desert/arid regions due to lack of soil water
4 301 content, sparse vegetation cover, and very low relative humidity above the surface. For
5 302 WBT, areas close to the coasts have higher values because they are more humid.
6 303 Increasing urbanization, evolving urban landscapes, and growing populations are
7 304 changing the land cover and the land-atmosphere energy fluxes exchanges. This paper
8 305 highlights two main points to be considered in designing future land use over this region:
9
10
11

12 306 1- LST and WBT change with the time of the day. The diurnal difference effect is
13 307 highlighted in Riyadh being a SUCI during the day, and a SUHI at night. For WBT, the
14 308 cities on the Persian Gulf have higher current and future WBT in early evenings of the
15 309 summer (air saturated with humidity), when people tend to go out. It is important to
16 310 consider these diurnal effects, to properly assess future climatic effects on LST and WBT
17 311 and their effect on outdoor activities at different times of the day.
18
19
20

21 312 2- Irrigation increases heat stress. Vegetated spaces can reduce the surface and near
22 313 surface temperatures through evapotranspiration and shade and is highlighted in many
23 314 studies as a strategy to reduce the intensities of SUHIs^{39,40}. However, vegetation in arid
24 315 regions requires irrigation and we show here that irrigation enhances the heat stress with
25 316 an increase in WBT reaching +2°C with respect to the surroundings (Figure 3). The
26 317 planned Saudi Green Initiative aims at planting 50 billion trees in Saudi Arabia
27 318 (<https://www.saudigreeninitiative.org/>). The choice of vegetation in populated region is
28 319 therefore important. For example, it is better to choose native or drought tolerant species
29 320 that requires less irrigation. Moreover, irrigation should be included in future climate
30 321 projections as it plays an essential role in determining future heat stress and survivability
31 322 in populated regions of the world.
32
33
34
35
36

37 323 The alarming future increase in temperatures in the Arabian Peninsula and shown in this
38 324 work would constrain major socio-economic development in cities on the Persian Gulf,
39 325 Gulf of Oman and the Red Sea. Even for the sustainable scenario, the high WBT poses
40 326 significant risk on outdoor activities and labor (such as constructing workers) even at night.
41 327 This region would considerably benefit from strict mitigation effort to reduce the severity
42 328 of the projected impact of climate change.
43
44
45

46 329 **Data access**

47 330 IASI land surface temperature (also called Earth's "skin temperature") data are available
48 331 on <https://iasi-ft.eu/>. ERA5 data (t2m, d2m, skin temperature/LST and surface pressure)
49 332 used in this work to calculate WBT are available from the Climate Data Store at the
50 333 following DOI: [10.24381/cds.adbb2d47](https://doi.org/10.24381/cds.adbb2d47).

51
52
53 334 EC-Earth3 model output prepared for CMIP6 ScenarioMIP are retrieved
54 335 here: <https://doi.org/10.22033/ESGF/CMIP6.727>
55

56 336
57
58
59
60

337 Acknowledgments

338 This project has received funding from the European Research Council (ERC) under the
339 European Union's Horizon 2020 and innovation programme (grant agreement No
340 742909). The IASI mission is a joint mission of Eumetsat and the Centre National d'Etudes
341 Spatiales (CNES, France). The IASI L1 data are distributed in near real time by Eumetsat
342 through the Eumetcast system distribution. The authors acknowledge the Aeris data
343 infrastructure for providing the IASI L1C data. The authors thank M. D. Boucher and D.
344 Coppens for the reprocessed L1C IASI radiances used to compute LST, and thank V.
345 Pellet, F. Aires, G. Levavasseur, Y.-W. Choi, and R. Döscher for useful discussions.

347 References

- 348 1. Masson-Delmotte, V., P. Zhai, A. Pirani, S.L., Connors, C. Péan, S. Berger, N.
349 Caud, Y. Chen, L. Goldfarb, M.I. Gomis, M. Huang, K. Leitzell, E. Lonnoy, J.B.R.,
350 Matthews, T.K. Maycock, T. Waterfield, O. Yelekçi, R. Yu, and B. Zhou. *IPCC,*
351 *2021: Climate Change 2021: The Physical Science Basis. Contribution of Working*
352 *Group I to the Sixth Assessment Report of the Intergovernmental Panel on Climate*
353 *Change.* Cambridge University Press. In Press.; 2021. Accessed August 12, 2021.
354 <https://www.ipcc.ch/assessment-report/ar6/>
- 355 2. Vogel MM, Orth R, Cheruy F, et al. Regional amplification of projected changes in
356 extreme temperatures strongly controlled by soil moisture-temperature feedbacks.
357 *Geophysical Research Letters.* 2017;44(3):1511-1519.
358 doi:<https://doi.org/10.1002/2016GL071235>
- 359 3. Pal JS, Eltahir EAB. Future temperature in southwest Asia projected to exceed a
360 threshold for human adaptability. *Nature Climate Change.* 2016;6(2):197-200.
361 doi:10.1038/nclimate2833
- 362 4. McKeown W, Bretherton F, Huang HL, Smith WL, Revercomb HL. Sounding the
363 Skin of Water: Sensing Air–Water Interface Temperature Gradients with
364 Interferometry. *J Atmos Oceanic Technol.* 1995;12(6):1313-1327.
365 doi:10.1175/1520-0426(1995)012<1313:STSOWS>2.0.CO;2
- 366 5. Good EJ. An in situ-based analysis of the relationship between land surface “skin”
367 and screen-level air temperatures. *Journal of Geophysical Research: Atmospheres.*
368 2016;121(15):8801-8819. doi:10.1002/2016JD025318
- 369 6. Rhee J, Im J, Carbone GJ. Monitoring agricultural drought for arid and humid
370 regions using multi-sensor remote sensing data. *Remote Sensing of Environment.*
371 2010;114(12):2875-2887. doi:10.1016/j.rse.2010.07.005
- 372 7. Zhou L, Dickinson RE, Tian Y, et al. A sensitivity study of climate and energy
373 balance simulations with use of satellite-derived emissivity data over Northern
374 Africa and the Arabian Peninsula. *Journal of Geophysical Research: Atmospheres.*
375 2003;108(D24). doi:10.1029/2003JD004083

- 1
2
3 376 8. Voogt JA, Oke TR. Thermal remote sensing of urban climates. *Remote Sensing of Environment*. 2003;86(3):370-384. doi:10.1016/S0034-4257(03)00079-8
4 377
5
6 378 9. Dialesandro JM, Wheeler SM, Abunnasr Y. Urban heat island behaviors in dryland
7 379 regions. *Environ Res Commun*. 2019;1(8):081005. doi:10.1088/2515-7620/ab37d0
8
9
10 380 10. Alahmad B, Tomasso LP, Al-Hemoud A, James P, Koutrakis P. Spatial Distribution
11 381 of Land Surface Temperatures in Kuwait: Urban Heat and Cool Islands. *Int J*
12 382 *Environ Res Public Health*. 2020;17(9). doi:10.3390/ijerph17092993
13
14 383 11. Abulibdeh A. Analysis of urban heat island characteristics and mitigation strategies
15 384 for eight arid and semi-arid gulf region cities. *Environ Earth Sci*. 2021;80(7):259.
16 385 doi:10.1007/s12665-021-09540-7
17
18 386 12. Song J, Du S, Feng X, Guo L. The relationships between landscape compositions
19 387 and land surface temperature: Quantifying their resolution sensitivity with spatial
20 388 regression models. *Landscape and Urban Planning*. 2014;123:145-157.
21 389 doi:10.1016/j.landurbplan.2013.11.014
22
23
24 390 13. Zhou W, Huang G, Cadenasso ML. Does spatial configuration matter?
25 391 Understanding the effects of land cover pattern on land surface temperature in
26 392 urban landscapes. *Landscape and Urban Planning*. 2011;102(1):54-63.
27 393 doi:10.1016/j.landurbplan.2011.03.009
28
29
30 394 14. Akbari H. Cooling our Communities. A Guidebook on Tree Planting and Light-
31 395 Colored Surfacing. Published online February 24, 2009. Accessed June 1, 2021.
32 396 <https://escholarship.org/uc/item/98z8p10x>
33
34 397 15. Mora C, Dousset B, Caldwell IR, et al. Global risk of deadly heat. *Nature Climate*
35 398 *Change*. 2017;7:501-506. doi:10.1038/nclimate3322
36
37
38 399 16. Raymond C, Matthews T, Horton RM. The emergence of heat and humidity too
39 400 severe for human tolerance. *Science Advances*. 2020;6(19).
40 401 doi:10.1126/sciadv.aaw1838
41
42 402 17. Sherwood SC, Huber M. An adaptability limit to climate change due to heat stress.
43 403 *PNAS*. 2010;107(21):9552-9555. doi:10.1073/pnas.0913352107
44
45 404 18. Clerbaux C, Boynard A, Clarisse L, et al. Monitoring of atmospheric composition
46 405 using the thermal infrared IASI/MetOp sounder. *Atmospheric Chemistry and*
47 406 *Physics*. 2009;9(16):6041-6054. doi:https://doi.org/10.5194/acp-9-6041-2009
48
49
50 407 19. Safieddine S, Parracho AC, George M, et al. Artificial Neural Networks to Retrieve
51 408 Land and Sea Skin Temperature from IASI. *Remote Sensing*. 2020;12(17):2777.
52 409 doi:10.3390/rs12172777
53
54
55
56
57
58
59
60

- 1
2
3 410 20. Clarisse L, Van Damme M, Gardner W, et al. Atmospheric ammonia (NH₃)
4 411 emanations from Lake Natron's saline mudflats. *Scientific Reports*. 2019;9(1):4441.
5 412 doi:10.1038/s41598-019-39935-3
6
7
8 413 21. de Foy B, Lu Z, Streets DG, Lamsal LN, Duncan BN. Estimates of power plant NO_x
9 414 emissions and lifetimes from OMI NO₂ satellite retrievals. *Atmospheric*
10 415 *Environment*. 2015;116:1-11. doi:10.1016/j.atmosenv.2015.05.056
11
12 416 22. Fioletov VE, McLinden CA, Krotkov N, Moran MD, Yang K. Estimation of SO₂
13 417 emissions using OMI retrievals. *Geophysical Research Letters*. 2011;38(21).
14 418 doi:https://doi.org/10.1029/2011GL049402
15
16 419 23. Bouillon M, Safieddine S, Hadji-Lazaro J, et al. Ten-Year Assessment of IASI
17 420 Radiance and Temperature. *Remote Sensing*. 2020;12(15):2393.
18 421 doi:10.3390/rs12152393
19
20
21 422 24. Davies-Jones R. An Efficient and Accurate Method for Computing the Wet-Bulb
22 423 Temperature along Pseudoadiabats. *Monthly Weather Review*. 2008;136(7):2764-
23 424 2785. doi:10.1175/2007MWR2224.1
24
25 425 25. Hersbach H, Bell B, Berrisford P, et al. The ERA5 global reanalysis. *Quarterly*
26 426 *Journal of the Royal Meteorological Society*. 2020;146(730):1999-2049.
27 427 doi:https://doi.org/10.1002/qj.3803
28
29
30 428 26. Döscher R, Acosta M, Alessandri A, et al. The EC-Earth3 Earth System Model for
31 429 the Climate Model Intercomparison Project 6. *Geoscientific Model Development*
32 430 *Discussions*. Published online February 11, 2021:1-90. doi:10.5194/gmd-2020-446
33
34 431 27. Eyring V, Bony S, Meehl GA, et al. Overview of the Coupled Model Intercomparison
35 432 Project Phase 6 (CMIP6) experimental design and organization. *Geoscientific*
36 433 *Model Development*. 2016;9(5):1937-1958. doi:10.5194/gmd-9-1937-2016
37
38
39 434 28. Riahi K, van Vuuren DP, Kriegler E, et al. The Shared Socioeconomic Pathways
40 435 and their energy, land use, and greenhouse gas emissions implications: An
41 436 overview. *Global Environmental Change*. 2017;42:153-168.
42 437 doi:10.1016/j.gloenvcha.2016.05.009
43
44 438 29. Aina YA, Adam EM, Ahmed F. Spationtemporal Variations in the Impacts of Urban
45 439 Land Use Types on Urban Heat Island effects: The Case of Riyadh, Saudi Arabia.
46 440 In: *The International Archives of the Photogrammetry, Remote Sensing and Spatial*
47 441 *Information Sciences*. Vol XLII-3-W2. Copernicus GmbH; 2017:9-14.
48 442 doi:10.5194/isprs-archives-XLII-3-W2-9-2017
49
50
51 443 30. Alshenaifi MA, Sharples S. A parametric analysis of the influence of wind speed
52 444 and direction on the thermal comfort performance of a Passive Draught
53 445 Evaporative Cooling (PDEC) system – field measurements from a Saudi Arabian
54 446 library. *IOP Conf Ser: Earth Environ Sci*. 2019;329:012042. doi:10.1088/1755-
55 447 1315/329/1/012042
56
57
58
59
60

- 1
2
3 448 31. Youssef AM, Abu Abdullah MM, Pradhan B, Gaber AFD. Agriculture Sprawl
4 449 Assessment Using Multi-Temporal Remote Sensing Images and Its Environmental
5 450 Impact; Al-Jouf, KSA. *Sustainability*. 2019;11(15):4177. doi:10.3390/su11154177
6
7 451 32. sdurayhem. Agricultural Production Survey Methodology. General Authority for
8 452 Statistics. Published September 29, 2019. Accessed January 3, 2022.
9 453 <https://www.stats.gov.sa/en/1060-0>
10
11 454 33. Al-Ghobari H, Dewidar AZ. A Comparative Study of Standard Center Pivot and
12 455 Growers-Based Modified Center Pivot for Evaluating Uniformity Coefficient and
13 456 Water Distribution. *Agronomy*. 2021;11(8):1675. doi:10.3390/agronomy11081675
14
15 457 34. Belmonte Rivas M, Stoffelen A. Characterizing ERA-Interim and ERA5 surface wind
16 458 biases using ASCAT. *Ocean Science*. 2019;15(3):831-852. doi:10.5194/os-15-831-
17 459 2019
18
19 460 35. Luo H, Ge F, Yang K, et al. Assessment of ECMWF reanalysis data in complex
20 461 terrain: Can the CERA-20C and ERA-Interim data sets replicate the variation in
21 462 surface air temperatures over Sichuan, China? *International Journal of Climatology*.
22 463 2019;39(15):5619-5634. doi:10.1002/joc.6175
23
24 464 36. Thomas SR, Nicolau S, Martínez-Alvarado O, Drew DJ, Bloomfield HC. How well
25 465 do atmospheric reanalyses reproduce observed winds in coastal regions of
26 466 Mexico? *Meteorological Applications*. 2021;28(5):e2023. doi:10.1002/met.2023
27
28 467 37. Simmons AJ, Willett KM, Jones PD, Thorne PW, Dee DP. Low-frequency variations
29 468 in surface atmospheric humidity, temperature, and precipitation: Inferences from
30 469 reanalyses and monthly gridded observational data sets. *Journal of Geophysical
31 470 Research: Atmospheres*. 2010;115(D1). doi:10.1029/2009JD012442
32
33 471 38. Dunn RJH, Willett KM, Ciavarella A, Stott PA. Comparison of land surface humidity
34 472 between observations and CMIP5 models. *Earth System Dynamics*. 2017;8(3):719-
35 473 747. doi:10.5194/esd-8-719-2017
36
37 474 39. Bowler DE, Buyung-Ali L, Knight TM, Pullin AS. Urban greening to cool towns and
38 475 cities: A systematic review of the empirical evidence. *Landscape and Urban
39 476 Planning*. 2010;97(3):147-155. doi:10.1016/j.landurbplan.2010.05.006
40
41 477 40. Wang ZH, Zhao X, Yang J, Song J. Cooling and energy saving potentials of shade
42 478 trees and urban lawns in a desert city. *Applied Energy*. 2016;161:437-444.
43 479 doi:10.1016/j.apenergy.2015.10.047
44
45
46
47
48
49
50
51
52
53
54
55
56
57
58
59
60

1
2
3
4
5
6
7
8
9
10
11
12
13
14
15
16
17
18
19
20
21
22
23
24
25
26
27
28
29
30
31
32
33
34
35
36
37
38
39
40
41
42
43
44
45
46
47
48
49
50
51
52
53
54
55
56
57
58
59
60

484
485
486

Accepted Manuscript